European Commission

JRC TECHNICAL REPORT

Modelling the tides on the North West European Shelf

Clare Coughlan
Adolf Stips

2015

Report EUR 27114 EN

Joint Research Centre

European Commission
Joint Research Centre
Institute for Environment and Sustainability

Contact information
Adolf Stips
Address: Joint Research Centre, Via Enrico Fermi 2749, TP 270, 21027 Ispra (VA), Italy
E-mail: adolf.stips@jrc.ec.europa.eu
Tel.: +39 0332 78 9876
Fax: +39 0332 78 5601

JRC Science Hub
https://ec.europa.eu/jrc

JRC93441

EUR 27114 EN

ISBN 978-92-79-45680-0 (PDF)

ISSN 1831-9424 (online)

doi:10.2788/17992

Luxembourg: Publications Office of the European Union, 2015

Abstract

Tides are a key process in the dynamics of the North West European Shelf. A GETM model has been developed for the region and this report describes the model performance. Measured harmonic constituents are compared with model outputs and these results are put into context with other shelf sea models of the region. Most of the differences between the model and observations are within the errors that are expected for a shelf sea model, and the overall statistics are skewed by poor performance in a few places. The major constituents are not represented particularly well in the Irish Sea, Celtic Sea and English Channel regions, but overall this model performs reasonably well, and better than many other shelf sea models of the region.

Contents

Introduction

The North West European Shelf is a broad temperate shelf forming the eastern margin of the Northern North Atlantic. It includes several shelf sea regions that are adjacent to the most populous and industrialized countries of Europe. The dynamics of the region are controlled by the seasonal heating cycle, atmospheric fluxes, tides, river inputs and exchanges with the open ocean. The region can largely be described as a seasonally stratified, downwelling shelf sea system (Holt et al., 2009) with a net inflow of surface waters and a net outflow on the sea floor across the shelf break into the deep Atlantic with a generally anti-clockwise circulation of the North Sea (Wakelin et al., 2008). The large scale ocean-shelf exchange is controlled by seasonal upwelling in the south of the region (Gomez-Gesteira et al., 2011), and the poleward slope current and Ekman transport in the North (Holt et al., 2009; Huthnance et al., 2009). Tidal mixing fronts separate the seasonally stratified from the well mixed/sporadically stratified shallower regions either nearer the coast or on banks and shoals. Although tides play a significant role in the circulation, horizontal density gradients play an important role, particularly during the summer and autumn months (Holt & Proctor, 2008).

The region is further characterized by two strong northward currents (the slope currents along the shelf break and the current along the Norwegian trench), that enclose the Northern part of the shelf. Local conditions in the area can be highly heterogeneous due to strong tidal dynamics, riverine inflow and the interface with the brackish waters of the Baltic Sea. Much of the open shelf is seasonally stratified; tidal mixing fronts separate stratified regions from well-mixed/sporadically stratified shallower regions. Tidal mixing fronts tend to separate nutrient-depleted from nutrient-rich waters, and cross frontal exchange processes can result in enhanced biological production (Pingree & Griffiths, 1982; Richardson & Visser, 2000), making these regions important for shelf sea coupled hydrodynamic ecosystem modelling. Since the extent of stratified regions is dependent on the local relationship between depth and tidal mixing (Simpson & Hunter, 1974), it is important that the model accurately reproduces the main tidal constituents. The vertical temperature structure, through its control over mixing, is crucial to the prediction of the vertical distribution of nutrients and contaminants, with consequent implications for biological and water quality modelling.

The North West European Shelf has some of the largest tides on the globe: for example, Avonmouth (Bristol Channel) has a spring tidal range of over 14 m (Pelling et al., 2013). The large tides make this one of the most energetic areas, with total dissipation rates approaching 200 GW (Egbert & Ray, 2001), which is about 5-6% of the total present-day global tidal dissipation. Tides across the region are dominated by the semi-diurnal constituents (in particular M_2 and S_2, with M_2 ca. 30-50% of S_2 according to Uehara et al., 2006). The predominantly semi-diurnal tides (Pingree & Griffiths, 1982) are a co-oscillating response of the shelf seas to the tides generated in the Atlantic Ocean. Tidal energy from the Atlantic is transmitted onto the European shelf into the Celtic Sea between Brittany and southern Ireland via the Atlantic semi-diurnal Kelvin wave, which travels south to north. The wave propagates into the English Channel and energy passes into the southern North Sea, the Irish Sea and into the Bristol Channel (Pugh, 1996). The north of Scotland diffracts part of the semi-diurnal wave, and it turns east and to the south into the North Sea. The diurnal tide behaves as a standing wave in the Celtic Sea, the Bristol Channel and English Channel, but without any tendency to resonance (Pugh, 1996). The tides in the North and Irish seas essentially behave like a Kelvin wave that enters from the North Atlantic, propagates along the UK coast, and is reflected at the end of each basin. The reflected wave then travels back on the opposite side of the basin (i.e. along the coast of continental Europe in the North Sea or the Irish Coast in the Irish Sea).

North West European Shelf GETM Model

The 3 minute x 3 minute North West European Shelf (NWES) hydrodynamic model is an implementation of the General Estuarine Transport Model, GETM (http://getm.eu, Burchard and Bolding, 2002; Stips et al., 2004). GETM is a three-dimensional free-surface primitive equation Arakawa C-grid (Arakawa & Lamb, 1977) model that uses the Boussinesq and boundary layer approximations. The Arakawa C-grid is known to be particularly prone to grid scale noise due to spatial averaging of Coriolis terms, but provided the deformation radius is well-resolved (~30 km), C-grid models yield the most accurate numerical solutions (Adcroft et al, 1999). The free-surface, density and active/passive tracers are located at the centre of the cell, whereas the horizontal velocities (*u* and *v*) are located at the west/east and south/north edges of the cell, respectively.

The model domain extends from the deep ocean to the coast from 46.4˚N to 63˚N and 17.5˚W to 13˚E and is divided into a 1/20˚ grid with (i, j) = (1, 1) at the south-west corner and dimensions (308, 347). The domain is large and the resolution is limited by the desire to be able to produce results in a reasonable time frame. Horizontal spherical coordinates and vertical, terrain-following σ-coordinates are combined to give a grid spacing of ~6 km resolution with 25 layers in the vertical. The σ-coordinates are equidistant for water depths shallower than 150 m, but in deeper water the levels are concentrated at the surface and the bed using a generalised version of the mixed–layer transformation proposed by (Burchard & Petersen, 1997), in order to better resolve the surface mixed layer and bottom boundary layer.

The internal Rossby radius in this domain might be expected to range from ~3 km in the river plumes to 10-20 km in the Norwegian Trench to ~30 km in the northeast Atlantic. This model is not expected to fully resolve the details of the on-shelf baroclinic features (such as frontal instabilities and river plumes), but it is hoped that their overall characteristics (such as frontal locations) are captured. Ideally the model would be of sufficient resolution to resolve both the internal and external radii, i.e. a resolution of the order <2 km, but at present the computational cost of such a system makes this impractical for coupled hydrodynamic-ecosystem modelling over an area of this extent.

A crucial issue with model development is balancing accuracy (how well the model reproduces in situ data) with respect to its ability to reproduce temporal trends (for example, how closely it reproduces the observed seasonal cycle. The North West European Shelf is an exceptionally data rich region and has been extensively modelled. Verification of the 3nm NWES model is achieved by comparison with a variety of observations, gridded products and other model simulations to evaluate its ability to reproduce instantaneous point values (and trends) and spatial characteristics (and trends). The model domain encompasses both open ocean and shelf sea regions, presenting a sizable challenge for any model.

Representation of tides in the model

Current and sea surface elevation within the model domain are driven by Flather boundary conditions (Flather, 1976; Carter & Merrifield, 2007). The Flather condition is a radiation boundary condition that combines the Sommerfield equation (with surface gravity wave phase speed) with a one-dimensional version of the continuity equation applied in the outwardly normal direction at an open boundary:

$$\bar{v}_n = \bar{v}_n^{ext} \pm \sqrt{\frac{g}{h}\left(\eta - \eta^{ext}\right)}$$

$\bar{v}_n^{ext}$ represents the external data, h is the local water depth and η, $\bar{u}$ and $\bar{v}$ are the prognostic variables prescribed along the boundary for the incoming wave. The differences between the external data and the model predictions are allowed to propagate out of the domain at the speed of the external gravity waves. Volume is conserved in the domain and variations due to physical forcing, such as tides, can be introduced through the external data. Since the open boundary condition involves only the depth-mean current, any current structure within the model is generated by the physics, i.e. primarily frictional effects (bed friction and internal friction). For each of the model open boundary points, hourly elevation and current data were derived from the Oregon State University inverse modelled netCDF gridded data set (Egbert & Erofeeva, 2002; http://volkov.oce.orst.edu/tides/). Hourly data were required, as with a greater timestep the data did not capture the full signal along the boundary, leading to an underestimation of the maximum elevations and velocities.

Experimental setup

The two main controls on the tides are the bathymetry and the bottom friction. Isolated cells were found to affect the tidal propagation through the model, so a large amount of work was put into adjusting the coastline to avoid the creation of 'lake' regions during wetting and drying. A range of values for the coefficient of bottom friction (z_0) was tested in the model to calibrate the tidal harmonics. The ability of the model to reproduce the tidal regime across the North West European Shelf is assessed by comparing the modelled harmonic constituents against those derived from observations at tide gauges and current measure, and FES2012 atlases (Finite Element Solutions), a tide model that includes data assimilation (Carrere et al., 2012; http://www.aviso.oceanobs.com/en/data/products/auxiliary-products/global-tide-fes.html). The harmonic constants from the tide gauge and current meter observations were extracted from the literature.

The FES2012 solution is obtained through the use of a finite-element hydrodynamic model that assimilates long-term altimetry data (Topex/Poseidon, Jason-1, Jason-2, ERS-1, ERS-2 and ENVISAT) and in situ harmonic data; although only 3 tide gauges have been assimilated so far for the European Shelf region. 32 tidal constituents are distributed on 1/16˚ grids (amplitude and phase). It is considered a fairly reliable reference in the deep ocean (Maraldi et al., 2013) and good results are obtained in shelf regions (Carrere et al., 2012).

Initial model runs were made using a constant bed roughness. These preliminary tests were run over 5 different bathymetries:

- B1: bathymetry base on NOOS
- B2: B1 depths increased by 5% throughout the domain
- B3: bathymetry base on GEBCO_08
- B4: B1 improved in coastal regions (drying 'lakes' removed)
- B5: B4 depths increased by 8% or a maximum of 5 m (where depths were greater than 62.6 m)

Davies & Aldridge (1993) examined the influence of small changes in water depth upon tidal elevations and currents in the Irish Sea. They found that an increase in water depth by a factor of 1.08 significantly improved the accuracy of the elevations and current magnitudes computed with a three-dimensional model. The justification for the increase in water depths is that depths from navigation charts tend to be biased towards minimum depths to avoid vessels going aground.

Observed values of friction coefficient range from 4.30×10^{-3} to $5.29 \pm 1.7 \times 10^{-3}$ (reported in Davies, 1986). Bed roughness values used in other European Shelf models range from 0.001 to 0.035 (see Table 1). These values are larger than the mean values for different bottom types reported in, for example, Soulsby, 1983. The larger values take into account the form drag over sand waves that cannot be resolved in larger grid models. No other models in this region have implemented a variable bed roughness. Bed roughness was varied from 0.001 to 0.008, corresponding to the sorts of values used in other shelf models and from observations. Initially, a spatially constant value of bed roughness was applied across the domain, but later tests were conducted with a spatially varying bed roughness to try to improve regions with a poor match between the model and observations. The overall statistics comparing the modelled harmonic elevation to those derived from observations are summarised by the Taylor diagrams (Taylor, 2001) shown in Figure 1 to Figure 5. While these runs were being completed, the GETM version was updated from 2.2 to 2.4. The naming convention for the runs is [bathymetry]_[z0 value]_[getm version].

Table 1: Values of z_0 used in other models

z_0	Reference	Region
0.0025	Xing et al. (2011); Davies et al. (1997)	European Shelf
0.003, 0.0025, 0.00125	Davies et al. (2011)	Celtic and Irish Sea
0.0035	Maraldi et al. (2013)	Iberia-Biscay-Ireland
0.005	Davies & Kwong (2000); Davies (1986)	European Shelf
0.015, 0.025, 0.035	Davies & Jones (1990)	European Shelf

Results

Taylor diagrams provide a summary of overall model performance, compared to the observations. The grey contours show the RMS errors and the dashed arc gives the observed standard deviation. The star shows the observed value. The distance from the origin to each model point is the standard deviation of the modelled amplitudes or phases; points closer to the origin than the dashed line underestimate the variance of the data, and those outside the dashed line overestimate this variance. In general the model captures the pattern of variation, with similar standard deviations between observed and modelled amplitudes and phases, except for the smaller constituents, where the magnitude of the spatial variability is either under- or over- represented in the model, depending on the model run. The major constituents (M_2 and S_2) have a high correlation with the phase and amplitude of the observed harmonic constituents, but the RMS errors are still fairly large. The bathymetries with the depth increase (B2, B5) gave the worst comparisons with M_2 amplitudes. Varying the bathymetry and/or the bottom roughness does not improve the match between the modelled and observed S_2 amplitudes, only increases or decreases the spatial variability between the points.

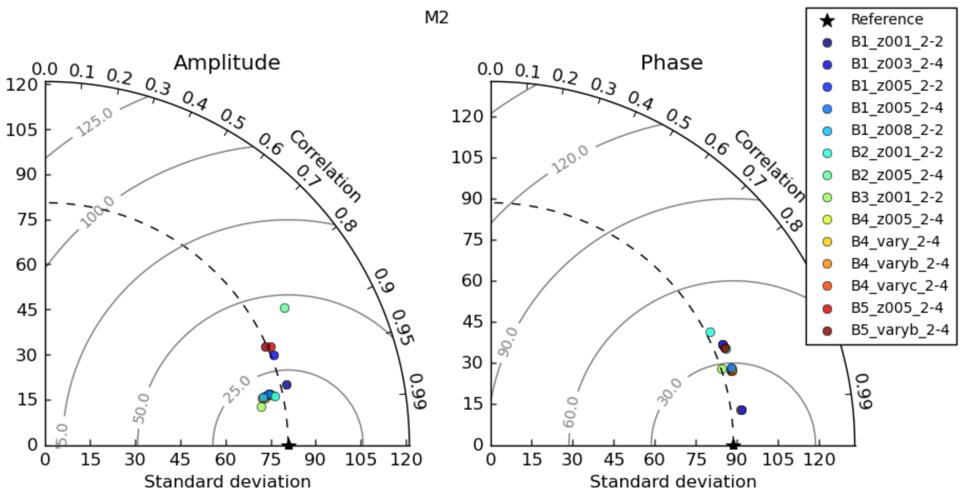

Figure 1: Taylor diagram showing the overall model performance for varying bathymetry, bed roughness and GETM version for the M_2 tidal amplitude (left) and phase (right)

Correlations are high, apart from the phase of the M_4 tide. The K_1 constituent is not particularly well-modelled. However, this is a small constituent (of the order of less than a few centimetres per second), so it is difficult to make meaningful comparisons. There is large spatial variability in the harmonic constituents, so the Taylor plots do not show any trends in model performance for tuning the bathymetry and bottom friction.

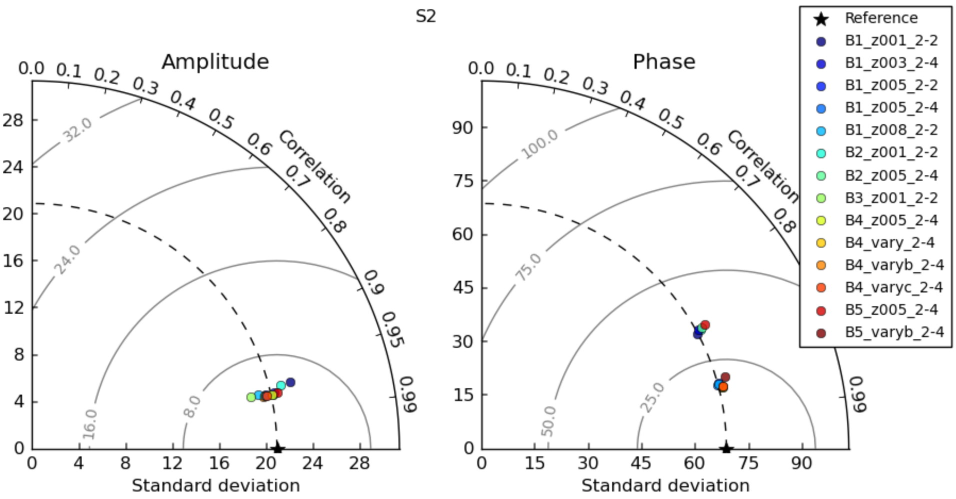

Figure 2: as for Figure 1, but the S_2 tide

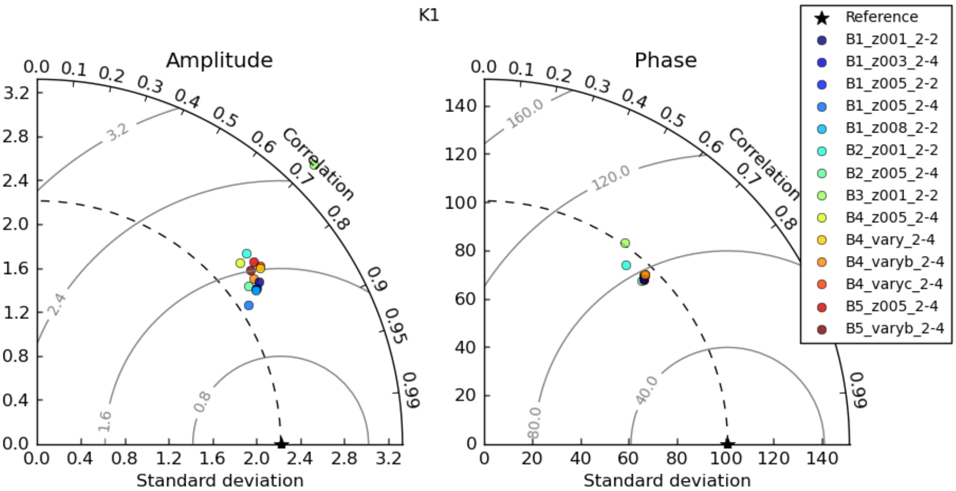

Figure 3: As for Figure 1, but the K_1 tide

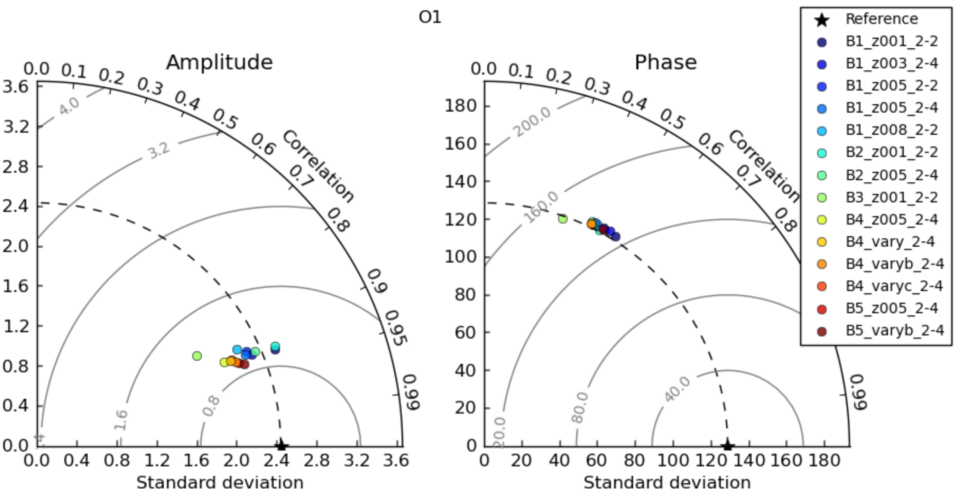

Figure 4: as for Figure 1, but the O_1 tide

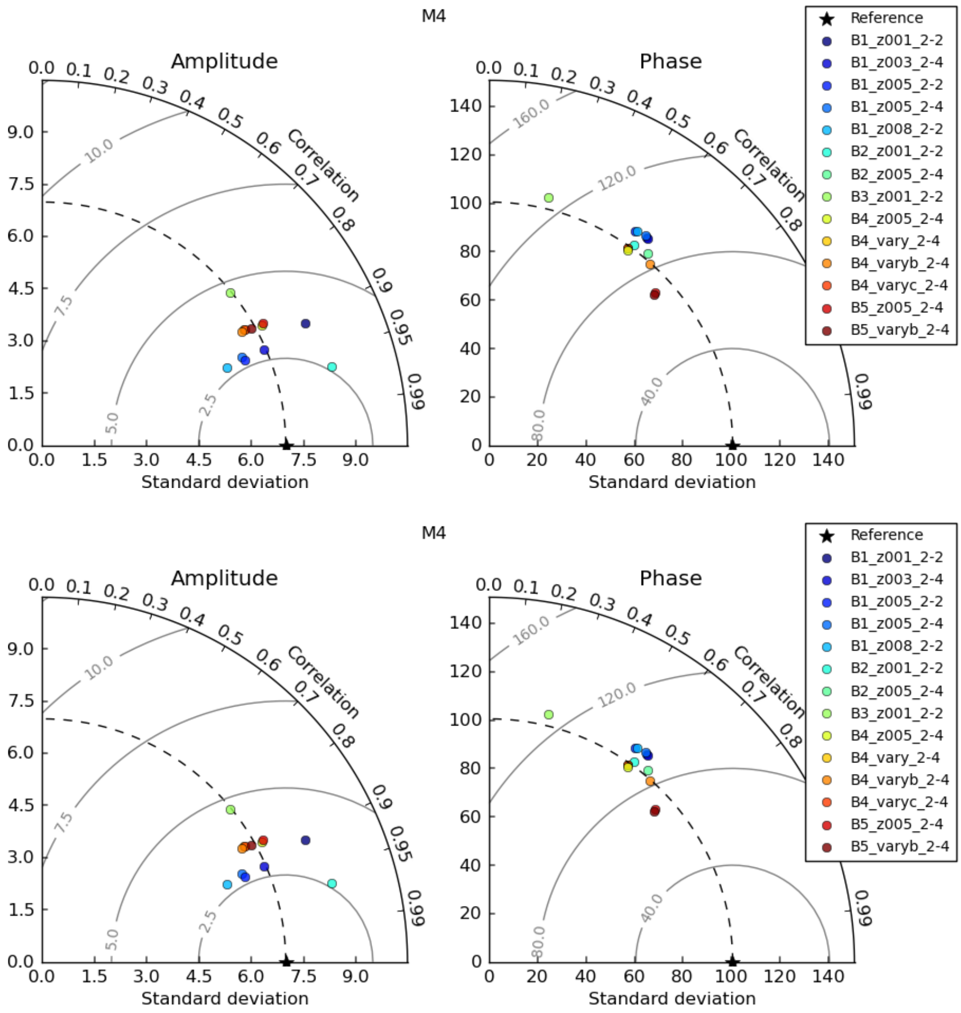

Figure 5: as for Figure 1, but the M_4 tide

Summary statistics were compared with other model runs found in the literature to assess the order of the errors. Table 2 gives a short summary of the models;

Table **3** shows the model statistics for the major diurnal constituents and Table 4 the major semi-diurnal statistics. The M_4 statistics are also shown in Table 4. This constituent is not forced at the boundary, but is calculated in the model due to bathymetric effects. Note that due to the different model resolutions and domains, not all of the comparisons below will have been with the same number of observations in exactly the same locations, but this comparison gives an idea of the order of the errors that are found in other European Shelf models.

Table 2: Tidally validated models found in the literature

Abbrv.	Reference	Short description
PD96	Proctor & Davies (1996)	B grid, σ-coords, POLCOMS
K97	Kwong et al. (1997)	C grid, 1/6°x 1/9°
H01	Holt et al. (2001)	B grid s-coords, POLCOMS, 1/6°x 1/9°
H05	Holt et al. (2005)	B grid, s-coords, POLCOMS, 1/10°x 1/7°
FOAM12	O'dea et al. (2012)	s-σ cords, NEMO, 1/15°x 1/9°
IBI13	Maraldi et al. (2013)	C grid, NEMO, 1/36°x 1/36°
C14	This model	C grid, GETM, 1/20°x 1/20°

Table 3 and Table 4 give the mean, RMS error and error in the complex plane (H_s). The mean error is simply the mean of the differences between the modelled and observed values. A positive value indicates model overestimation and a negative value is model underprediction. The root mean square error (RMSE) gives an idea of the size of the model errors in physical terms:

$$RMSE = \sqrt{\frac{\sum_{i=1}^{n}\left(M_i - O_i\right)^2}{n}}$$

n is the number of data points and O_i and M_i are observed and modelled values, respectively. H_s combines both amplitude and phase error into a single error measurement (Kwong et al., 1997).

$$H_s = \frac{1}{n}\sum_{i=1}^{n}\left(C_i^2 + S_i^2\right)^{\frac{1}{2}}$$

$$C_i = h_0 \cos(g_0) - h_c \cos(g_c)$$

$$S_i = h_0 \sin(g_0) - h_c \sin(g_c)$$

h_0, g_0 and h_c, g_c are the observed and computed amplitude and phase at each gauge, and n is the number of locations where observational data are available.

Table 3: A comparison of modelled diurnal tidal constituents with tide gauge measurements. Statistics are from model minus observed values of amplitude (h cm) and phase (g˚). H_s is the error in the complex plane (cm) defined in Kwong et al. (1997)

Statistic	Model	Q1		O1		K1	
		h	g	h	g	h	g
Mean	PD96	-0.40	12.7	-2.00	3.7	1.60	-16.4
	K97	-0.90	3.3	-1.50	-6.4	-0.70	-11.5
	H01	-0.41	10.2	-1.96	-5.6	2.95	-19.3
	H05	0.00	-	2.00	-	-1.30	-
	FOAM12	-	-	-1.30	-2.2	-0.20	-8.4
	This model	-0.32	-11.4	-0.45	-10.2	0.66	5.47
RMS	PD96	6.97	42.25	2.74	20.67	2.92	34.49
	K97	6.98	39.60	2.22	24.20	1.88	26.30
	H01	6.97	42.12	2.68	24.10	4.23	36.50
	H05	6.8	-	2.60	-	2.40	-
	FOAM12	-	-	1.90	15.70	1.80	17.70
	This model	0.60	27.74	1.10	29.31	1.80	21.25
H_s	PD96	1.90		3		4.3	
	K97	1.60		2.7		2.8	
	H01	1.92		3.08		5.53	
	FOAM12	-		1.30		1.8	
	This model	0.89		1.89		2.33	

Table 4: A comparison of modelled semi-diurnal tidal constituents with tide gauge measurements. Statistics are from model minus observed values of amplitude (h cm) and phase (g°). H_s is the error in the complex plane (cm) defined in Kwong et al. (1997)

Statistic	Model	N2		M2		S2		M4	
		h	g	h	g	h	g	h	g
Mean	PD96	1.5	-3.6	-3.3	1.3	0.9	-3.8	-0.5	26.3
	K97	-0.1	-11.1	-2.4	-2.4	-1.5	-9.5	-1.5	0.6
	H01	1.44	-5.48	4.99	1	3.83	-5.31	1.33	26.3
	H05	-1.6	-	-1.9	-	-1.7	-	-1.8	-
	FOAM12	0.4	2.7	-4.7	-0.2	-0.4	0.5	-	-
	This model	0.08	-1.91	-0.1	-3.2	0.28	-3.55	-0.85	8.28
RMS	PD96	4.5	26.04	14.25	14.99	6.54	22.3	4.7	82.17
	K97	3.9	28.9	12.7	17.3	7.32	25.1	5.48	80.9
	H01	4.52	26.68	14.9	14.76	7.64	22.55	5.38	82.55
	H05	4.6	-	16.3	-	7.3	-	5.0	-
	FOAM12	2.9	21.6	10.3	14.7	3.7	12.8	-	-
	This model	2.8	16.14	18.0	13.4	4.6	17.90	3.6	48.52
H_s	PD96	6.9		21.1		11.2		5.9	
	K97	5.9		16.6		10.2		5.4	
	H01	6.79		21.61		12.04		6.84	
	IBI13	-		21.6		8.0		7.1	
	This model	3.98		19.85		6.99		4.15	

As seen in Table 3 and Table 4, the model errors are typical for models of this region. The RMS error for the M_2 elevation is higher than for other models, but the phase is better modelled, which give a better overall H_s value. The M_4 tide, which is not forced on the boundary, but produced through interaction of the M_2 with the bathymetry, is modelled much better in this model than in other shelf models. In fact, all constituents are modelled better than other shelf models, apart from K_1, which is a minor constituent with very small amplitudes. Errors of the order shown here in the diurnal tides are to be expected, and relate to the accuracy with which these constituents can be measured.

The Taylor plots only give an impression of how the model is performing overall, and spatial plots are used to determine where the model is performing well and where it can be improved. Amphidromes represent the nodes of standing waves in a rotating system, and are formed by the interaction of incident and reflected Kelvin waves. Their position is affected by water depth, frictional effects and topography, and the model does a good job of predicting their locations. The semi-diurnal constituents give similar co-tidal patterns (Figure 6), although the M_2 tide has by far the largest amplitudes. There is a degenerate amphidromic point at the southern tip of Norway with an amphidromic point off the west coast of Denmark and another in the Southern Bight of the North Sea. The amphidromic points between Scotland and Northern Ireland and off south-east Ireland are degenerate. The pattern in the semi-diurnal co-tidal charts (Figure 6) shows larger spatial variability than that found for the diurnal tides (Figure 7) as a result of the shorter wavelength of these components. The diurnal co-tidal charts (Figure 7) are characterised by an amphidromic point off the south-west corner of Norway with tidal amplitudes increasing to the south-west of this point.

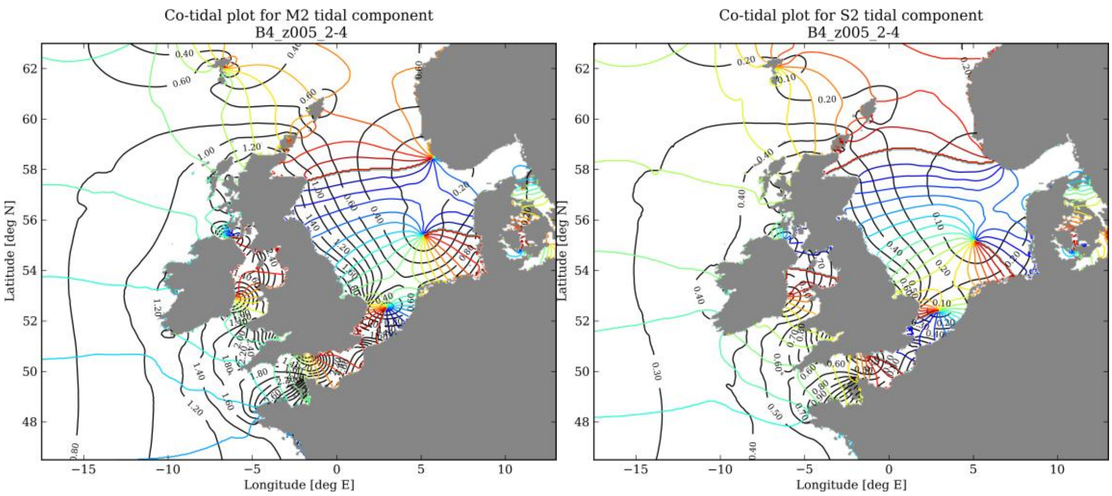

Figure 6: Co-tidal plots for the major harmonic constituents, M_2 (left) and S_2 (right). The labelled black lines give the tidal elevation and the coloured lines the phase

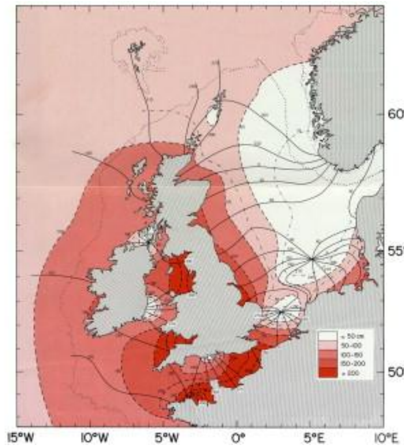

Figure 7: Co-tidal chart for the M2 tidal constituent based solely on observational data from tide gauges and bottom pressure sensors (from Howarth, 1990). The dashed lines with values are lines of constant amplitude (m); solid lines indicate lines of constant phase

Figure 6 demonstrates that the model reproduces the expected pattern of propagating tidal waves around amphidromic points, with similarities in the spatial variation to that found in other shelf-wide models (O'dea et al., 2012; Holt et al., 2005; S. C. M. Kwong et al., 1997) and observations (Howarth, 1990, see Figure 7). In particular, the degenerate amphidrome south of Norway that has proven to be difficult to obtain in other modelling studies (O'dea et al., 2012) is well-modelled. Figure 8 shows the location of this point in the FOAM and POLCOMS models (O'dea et al., 2012). The amphidromic point off Norway is displaced offshore (westwards) for decreasing z_0 (not shown here), but there is no significant change in the location of the other amphidromic points for changing z_0. The increase in amplitudes from ocean to shelf and within the English Channel and Southern Bight of the North Sea is clearly evident.

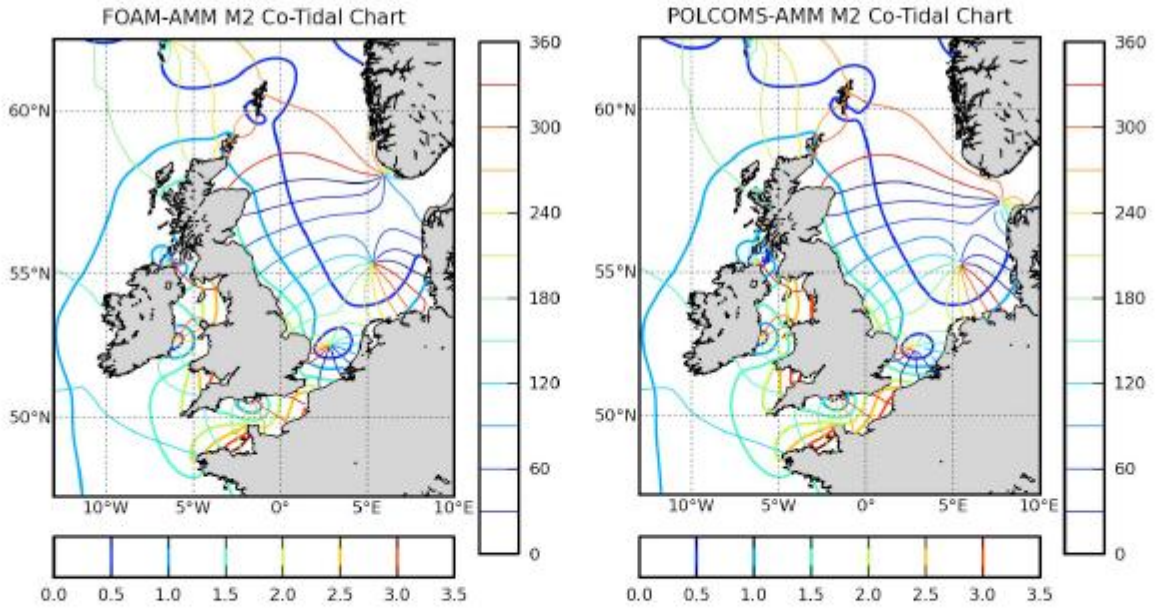

Figure 8: M2 co-tidal chart for FOAM12 (left) and POLCOMS (right). Taken from O'Dea et al., 2012

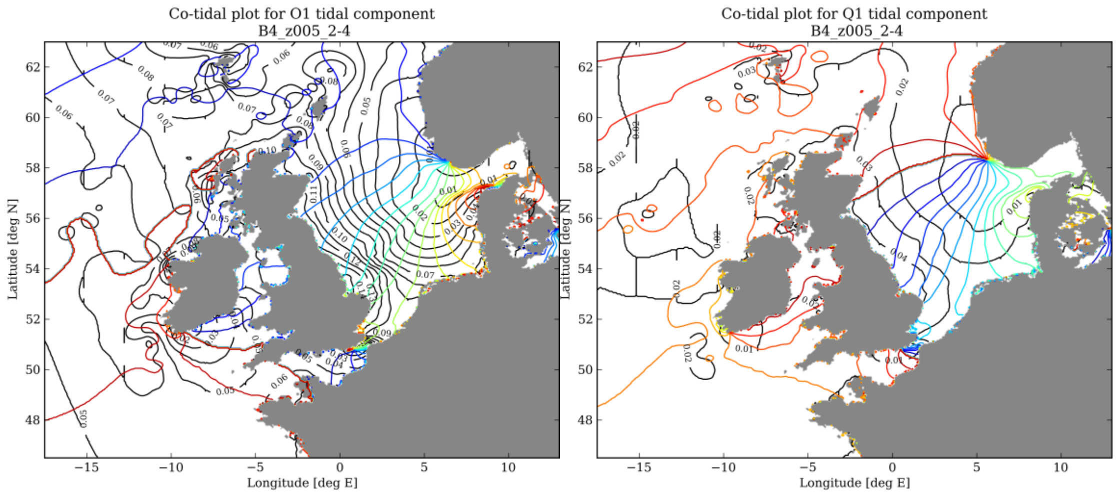

Figure 9: As for Figure 6, but for the major diurnal constituents, Q_1 (left) and O_1 (right)

The errors are not distributed evenly across the domain. In Figure 10 to Figure 14 the filled contours show the differences between modelled output and the FES2012 atlas and the coloured circles give differences between modelled output and tide gauges (the scale is the same and these are absolute values of model – observation, where blue indicates model underprediction and red is model overprediction). The tides tend to be well modelled in the open sea regions (for example, Figure 13), however, there is an overprediction in the Celtic Sea, western English Channel, the North Channel approach to the Irish Sea and the Baltic, and an underprediction in the Irish Sea.

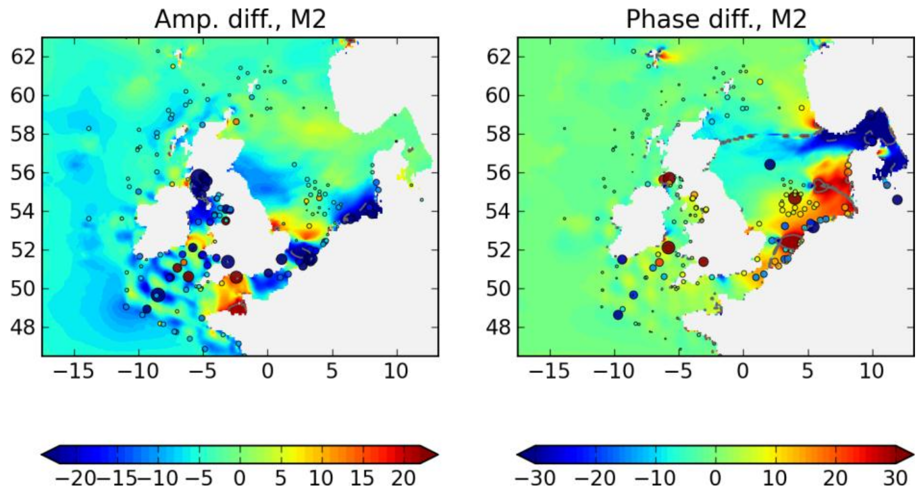

Figure 10: Distribution of errors from a comparison of M_2 elevation amplitude (left) and phase (right) for the B3 GEBCO_08 bathymetry (6 months harmonic analysis); z_0 = 0.001

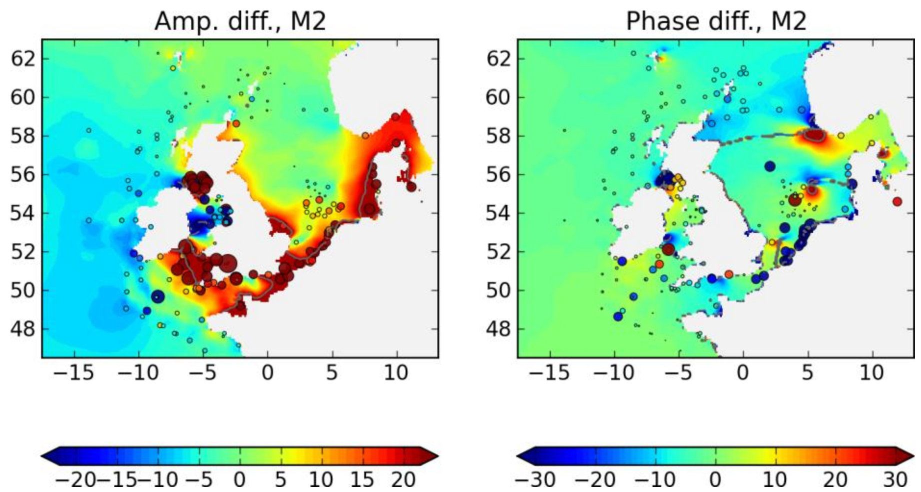

Figure 11: Distribution of errors from a comparison of M_2 elevation amplitude (left) and phase (right) for the B1 NOOS bathymetry (6 months harmonic analysis); z_0 = 0.001

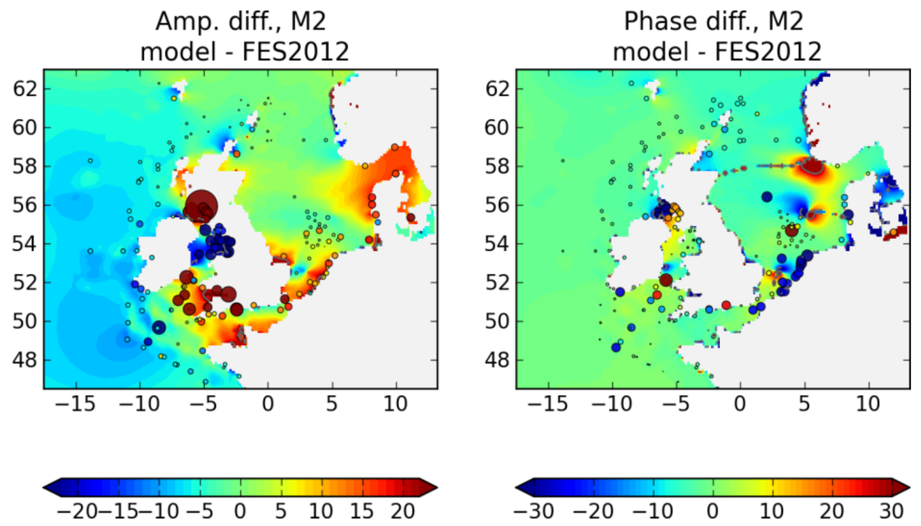

Figure 12: Distribution of errors from a comparison of M_2 elevation amplitude (left) and phase (right) for the B1 NOOS bathymetry (6 months harmonic analysis), z_0 = 0.003

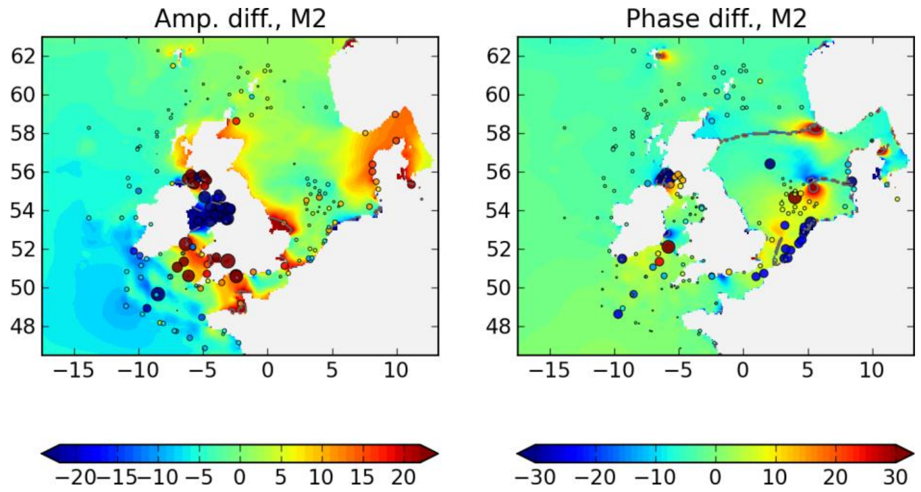

Figure 13: Distribution of errors from a comparison of M2 elevation amplitude (left) and phase (right) for the B1 NOOS bathymetry (6 months harmonic analysis), z0 = 0.005

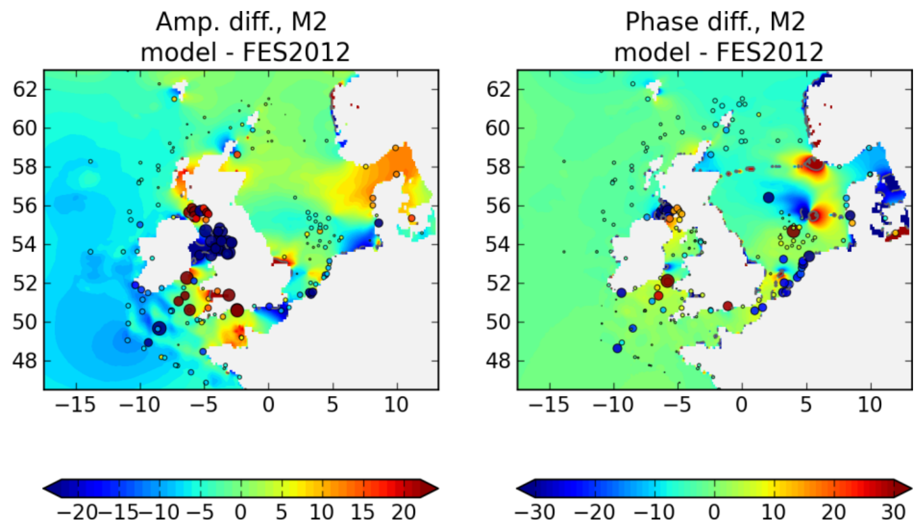

Figure 14: Distribution of errors from a comparison of M2 elevation amplitude (left) and phase (right) for the B1 NOOS bathymetry (6 months harmonic analysis), z0 = 0.008

A large part of the of the mean amplitude error for M_2 is due to an underestimation of the M_2 amplitude in the Irish sea, as found in other shelf models (for example, O'Dea et al., 2012). The Irish and Celtic Seas are particularly problematic with underestimation of the M_2 tide in the Irish Sea and overestimation in the approaching channels (North Channel and St George's Channel). This may be due to a number of factors, including errors in boundary input and bathymetry, dissipation being too strong in regions of underestimation, or too weak in regions of overestimation. The model grid may be too coarse to resolve regions such as the North Channel and Bristol Channel.

The GEBCO_08 bathymetry produces reasonable statistics overall (the best overall statistics for all the runs with spatially constant z_0, and Figure 10 shows that the model matches the observations in many regions. The Skagerrak region is much better modelled than for the NOOS bathymetry (for example, Figure 11). However, most of the English Channel and Celtic Sea (where there are no observations) is poorly modelled and there are much larger phase differences than seen when using the NOOS bathymetry.

With the NOOS bathymetry, the model tends to overpredict tidal elevations in the western English Channel and Celtic Sea, the northern approaches to the Irish Sea and the Skagerrak region. Elevations in the Irish Sea are underpredicted. The phase is reasonably well-modelled, but the wave tends to be travelling too slowly along the German and Dutch coastline. A bottom friction of 0.001 is too low, and the elevations are overpredicted for most of the coastal parts of the domain. Varying z_0 does not have much effect on the phase, which is fairly well represented across the domain. None of the values tested improve the issue of underprediction in the Irish Sea, but a constant value of 0.005 gives the best representation across the domain. These are the values shown in Table 3 and Table 4, and although the RMSE for M_2 elevations is slightly larger than other shelf models, all the other constituents are modelled better. A full set of statistics for the model run with $z_0 = 0.005$ is shown in Table 5 and Table 6.

Table 5: Modelled statistics for semi-diurnal tidal elevations for the NOOS bathymetry with $z_0 = 0.005$

Statistic	M_2		S_2		M_4	
	h	g	h	g	h	g
RMSE	18.00	13.35	4.60	17.90	3.60	48.52
Reliability index	1.29	1.75	1.19	1.18	2.09	2.95
NSME	0.95	0.98	0.95	0.93	0.74	0.77
pbias	-0.04	-1.65	0.87	-1.79	-10.97	3.96
Cost function	-0.00	-0.04	0.01	-0.05	-0.12	0.08
Corr coeff	0.98	0.95	0.98	0.97	0.88	0.58

Table 6: Modelled statistics for diurnal tidal elevations for the NOOS bathymetry with z0 = 0.005

Statistic	K_1		O_1	
	h	g	h	g
RMSE	1.80	21.25	1.10	29.31
Reliability index	1.41	30.16	1.35	4.56
NSME	0.33	0.95	0.79	0.95
pbias	10.13	-3.24	-7.20	5.18
Cost function	0.30	-0.05	-0.19	0.08
Corr coeff	0.74	0.69	0.91	0.43

Table 7: RMS error of the complex amplitude difference between observed and modelled tidal components for the sea surface elevation. Units are in cm. The Irish Sea is delimited by 51˚N–56˚N, 9˚W-3˚W; the English Channel is delimited by 48.5˚N-51.5˚N; the North Sea region is delimited by 51.5˚N-60˚N, 4.5˚W-7.5˚E; and the Baltic region is delimited by 56˚N-59˚N, 7.5˚E-13˚E. Maraldi et al. (2013) examined these same regions, although their model covers a much wider region.

Region	Model run	M2	S2	K1	O1	M4
Whole domain	Maraldi *et al.*, (2013)	21.6	8.0	1.8	1.3	7.1
	z_0 = 0.005	19.85	6.99	2.33	1.89	4.15
	varyz_0	19.73	7.00	2.42	1.91	4.17
	varyz_0b	20.08	7.01	2.24	1.94	4.14
	varyz_0c	20.13	7.01	2.43	1.92	4.17
Irish Sea	Maraldi *et al.*, (2013)	25.9	10.1	1.7	1.3	11.1
	z_0 = 0.005	32.30	16.10	2.23	2.60	4.32
	varyz_0	32.59	15.70	2.28	2.64	4.42
	varyz_0b	33.87	15.83	2.24	2.69	4.34
	varyz_0c	33.90	15.80	2.28	2.66	4.43
English Channel	Maraldi *et al.*, (2013)	23.6	8.1	1.5	1.9	7.5
	z_0 = 0.005	39.67	15.13	1.71	1.86	9.70
	varyz_0	36.82	15.77	1.78	1.89	10.15
	varyz_0b	36.81	14.89	1.91	1.85	10.20
	varyz_0c	37.29	15.66	1.76	1.88	10.15
North Sea	Maraldi *et al.*, (2013)	14.7	4.7	2.7	1.0	6.2
	z_0 = 0.005	20.17	4.37	2.84	1.98	4.26
	varyz_0	20.90	4.42	2.94	1.98	4.20
	varyz_0b	21.52	4.34	2.65	1.95	4.12
	varyz_0c	21.26	4.41	2.94	1.98	4.20
Baltic Sea	Maraldi *et al.*, (2013)	29.8	9.0	2.4	2.1	0.9
	z_0 = 0.005	13.5	2.95	0.30	1.13	2.71
	varyz_0	13.45	3.05	1.45	1.27	2.57
	varyz_0b	10.35	2.56	1.17	1.48	2.35
	varyz_0c	13.15	3.02	1.44	1.26	2.54

Tests were made with varying the bed roughness to try to improve the model results in the Celtic Sea and the English Channel (not shown here). This did not lead to significant changes in the overall patterns and tidal elevations in the Irish Sea are still underpredicted. A spatially constant $z_0 = 0.005$ gives the best overall match with observations.

Table 7 gives a regional comparison of the RMS of the complex difference (Kwong et al., 1997) for each tidal constituent. To appreciate how significant these errors are, they are compared with overlapping regions assessed by Maraldi et al. (2013). Note however, that the measurement points differ between this study and that of Maraldi et al. (2013). Overall this model performs reasonably well, but the major constituents are not represented particularly well in the Irish Sea, Celtic Sea and English Channel regions. No solution has yet been found to improve the model performance in these regions.

Most of the differences between the model and observations are within the errors that are expected for a shelf sea model, and the overall statistics are skewed by poor performance in a few places. This model performs much better than the FES2012 model for the M_4 constituent. This is to be expected due to the better representation of coastal regions in our finer resolution model. There is still an underprediction of the M_4 tide by this model, suggesting that the advective terms in near-shore regions are still not well-represented. In particular, the phase of the M_4 tide is not well-matched with the observations.

Conclusions

A three dimensional hydrodynamic GETM model has been set up for the North West European Shelf. This is a tidally important region, where tidal motions provide the dominant source of energy and therefore tides play a key role in the development of the water column properties. Model validation is essential to illustrate the potential use of this model to capture the wide variety of processes and scales across the shelf region, and the 3nm NWES GETM model has been shown to capture the complicated tidal dynamics of this region. In a few regions (Irish Sea, Celtic Sea and English Channel), the major tidal constituents are not well-represented, but for most of the shelf region the model performs well within the errors that are expected for a shelf sea model. The analysis of the tidal elevations and current fields show that bathymetry is the main control on tidal wave propagation; small errors in the bathymetry (depth and slope) can generate large displacements in the circulation patterns. Further work should focus on improving the local bathymetry in the Irish Sea, Celtic Sea and English Channel regions. Overall, this model has been shown to have a good representation of the tides across the shelf and is therefore provides a good tool for further studies in the region.

References

Arakawa, A. & Lamb, V.R., 1977. Computational design of the basic dynamical processes of the UCLA General Circulation Model. *Meth. Comput. Phys.*, pp.173–263.

Adcroft, A.J., Hill, C.N. and Marshall, J.C., 1999. A new treatment of the coriolis terms in C-Grid models at both high and low resolutions. Monthly Weather Review, 127, pp. 1928 - 1936.

Burchard, H. & Bolding, K., 2002. *GETM -- a general estuarine transport model. Scientific Documentation*,

Burchard, H. & Petersen, O., 1997. Hybridisation between σ and z coordinates for improving the internal pressure gradient calculation in marine models with steep bottom slopes. *Int. J. Numer. Meth. Fluids*, 25, pp.1003–1023.

Carrere, L. et al., 2012. FES2012: A new global tidal model taking advantage of nearly 20 years of altimetry. In *Proceedings of meeting "20 years of altimetry"*.

Carter, G.S. & Merrifield, M.A., 2007. Open boundary conditions for regional tidal simulations. *Ocean Modelling*, 18, pp.194–209.

Davies, A. & Kwong, S., 2000. Tidal energy fluxes and dissipation on the European continental shelf. *Journal of Geophysical Research: …*, 105(C9), pp.21969–21989. Available at: http://onlinelibrary.wiley.com/doi/10.1029/2000JC900078/full.

Davies, A.M., 1986. A Three-Dimensional Model of the Northwest European Continental Shelf, with Application to the M4 Tide. *J. Phys. Oceanogr.*, 16, pp.797–813.

Davies, A.M. & Aldridge, J.N., 1993. A numerical model study of parameters influencing tidal currents in the Irish Sea. *Journal of Geophysical Research*, 98. Available at: http://dx.doi.org/10.1029/92JC02890.

Davies, A.M. & Jones, J.E., 1990. Application of a three-dimensional turbulence energy model to the determination of tidal currents on the Northwest European shelf. *Journal of Geophysical Research*, 95(C10), pp.18143–18162.

Davies, A.M., Jones, J.E. & Xing, J., 1997. Review of Recent Development in Tidal Hydrodynamic Modelling. I: Spectral Models. *Journal of Hydraulic Engineering*, pp.230–278.

Davies, A.M., Xing, J. & Jones, J.E., 2011. A model study of tidal distributions in the Celtic and Irish Sea regions determined with finite volume and finite element models. *Ocean Dynamics*, 61. Available at: http://dx.doi.org/10.1007/s10236-011-0428-1.

Egbert, G.D. & Erofeeva, S.Y., 2002. Efficient inverse modeling of barotropic ocean tides. *J Atmos Oceanic Technol*, 19(2), pp.183–204.

Egbert, G.D. & Ray, R.D., 2001. Estimates of M2 tidal energy dissipation from TOPEX/Poseidon altimiter data. *Journal of Geophysical Research*, 106(C10), pp.22475–22502.

Flather, R.A., 1976. A tidal model of the northwest European continental shelf. *Memoires de la Societe Royale de Sciences de Liege*, 10(6), pp.141–164.

Gomez-Gesteira, M. et al., 2011. Coastal processes in northwestern Iberia, Spain. *Continental Shelf Research*, 31(5), pp.367–375.

Holt, J., James, I. & Jones, J., 2001. An s coordinate density evolving model of the northwest European continental shelf: 2. Seasonal currents and tides. *Journal of Geophysical Research:* 106. Available at: http://onlinelibrary.wiley.com/doi/10.1029/2000JC000303/full.

Holt, J. & Proctor, R., 2008. The seasonal circulation and volume transport on the northwest European continental shelf: A fine-resolution model study. *Journal of Geophysical Research*, 113(C6), p.C06021. Available at: http://doi.wiley.com/10.1029/2006JC004034.

Holt, J., Wakelin, S. & Huthnance, J., 2009. Down-welling circulation of the northwest European continental shelf: A driving mechanism for the continental shelf carbon pump. *Geophysical Research Letters*, 36(14), p.L14602. Available at: http://doi.wiley.com/10.1029/2009GL038997.

Holt, J.T. et al., 2005. Error quantification of a high-resolution coupled hydrodynamic–ecosystem coastal–ocean model: Part 1 model overview and assessment of the hydrodynamics. *Journal of Marine Systems*, 57(1-2), pp.167–188. Available at: http://linkinghub.elsevier.com/retrieve/pii/S0924796305001053.

Howarth, M.J., 1990. Atlas of tidal elevations and currents around the British Isles.

Huthnance, J.M., Holt, J.T. & Wakelin, S.L., 2009. Deep ocean exchange with west-European shelf seas Deep ocean exchange with west-European shelf seas. *Ocean Science*, 5, pp.621–634.

Kwong, S., Davies, A. & Flather, R., 1997. A three-dimensional model of the principal tides on the European shelf. *Progress in Oceanography*, 39(97), pp.205–262. Available at: http://www.sciencedirect.com/science/article/pii/S0079661197000141.

Kwong, S.C.M., Davies, A.M. & Flather, R.A., 1997. A three-dimensional model of the principal tides of the European shelf. *Progress in Oceanography*, 39, pp.205–262.

Maraldi, C. et al., 2013. NEMO on the shelf: assessment of the Iberia–Biscay–Ireland configuration. *Ocean Science*, 9(4), pp.745–771. Available at: http://www.ocean-sci.net/9/745/2013/.

O'dea, E. et al., 2012. An operational ocean forecast system incorporating NEMO and SST data assimilation for the tidally driven European North-West shelf. *Journal of Operational Oceanography*, 5(1), pp.3–17. Available at: http://www.ingentaconnect.com/content/imarest/joo/2012/00000005/00000001/art00002.

Pelling, H.E., Mattias Green, J. a. & Ward, S.L., 2013. Modelling tides and sea-level rise: To flood or not to flood. *Ocean Modelling*, 63, pp.21–29. Available at: http://linkinghub.elsevier.com/retrieve/pii/S1463500312001813.

Pingree, R.D. & Griffiths, D.K., 1982. Tidal Friction and the Diurnal Tides on the North-West European Shelf. *Journal of the Marine Biological Association of the United Kingdom*, 62(03), pp.577–593. Available at: http://journals.cambridge.org/article_S0025315400019767.

Proctor, R. & Davies, A.M., 1996. A three dimensional hydrodynamic model of tides off the north-west coast of Scotland. *Journal of Marine Systems*, 7(1), pp.43–66.

Pugh, D.T., 1996. *Tides, surges and mean sea level*, Wiley, New York.

Richardson, K. & Visser, A., 2000. Subsurface phytoplankton blooms fuel pelagic production in the North Sea. Available at: http://dx.doi.org/10.1093/plankt/22.9.1663.

Simpson, J.H. & Hunter, J.R., 1974. Fronts in the Irish Sea. *Nature*, pp.404–406.

Stips, A. et al., 2004. Simulating the temporal and spatial dynamics of the {N}orth {S}ea using the new model GETM (General Estuarine Transport Model). *Ocean Dynamics*, 54(2), pp.266–283. Available at: http://link.springer.com/10.1007/s10236-003-0077-0.

Taylor, K., 2001. Summarizing multiple aspects of model performance in a single diagram. *Journal of Geophysical Research: Atmospheres* 106, pp.7183–7192. Available at: http://onlinelibrary.wiley.com/doi/10.1029/2000JD900719/full.

Uehara, K. et al., 2006. Tidal evolution of the northwest European shelf seas from the Last Glacial Maximum to the present. *Journal of Geophysical Research*, 111(C9), p.C09025. Available at: http://doi.wiley.com/10.1029/2006JC003531.

Wakelin, S.L., Holt, J.T. & Proctor, R., 2008. The influence of initial conditions and open boundary conditions on shelf circulation in a 3D ocean-shelf model of the North East Atlantic. *Ocean Dynamics*, 59(1), pp.67–81. Available at: http://link.springer.com/10.1007/s10236-008-0164-3.

Xing, J., Davies, A.M. & Jones, J.E., 2011. Application of an unstructured mesh model to the determination of the baroclinic circulation of the Irish Sea. *Journal of Geophysical Research*, 116(C10), p.C10026. Available at: http://doi.wiley.com/10.1029/2011JC007063.

European Commission
EUR 27114 EN – Joint Research Centre – Institute for Environment and Sustainability

Title: **Modelling the tides on the North West European Shelf**

Authors: Clare Coughlan, Adolf Stips

Luxembourg: Publications Office of the European Union

2015 – 25 pp. – 21.0 x 29.7 cm

EUR – Scientific and Technical Research series – ISSN 1831-9424 (online)

ISBN 978-92-79-45680-0 (PDF)

doi: 10.2788/17992

LB-NA-27114-EN-N

JRC Mission

As the Commission's in-house science service, the Joint Research Centre's mission is to provide EU policies with independent, evidence-based scientific and technical support throughout the whole policy cycle.

Working in close cooperation with policy Directorates-General, the JRC addresses key societal challenges while stimulating innovation through developing new methods, tools and standards, and sharing its know-how with the Member States, the scientific community and international partners.

Serving society
Stimulating innovation
Supporting legislation

doi:10.2788/17992

ISBN 978-92-79-45680-0

Publications Office